Sains Malaysiana 49(1)(2020): 57-67
http://dx.doi.org/10.17576/jsm-2020-4901-07

Adsorption of Para Nitro-phenol by Activated Carbon produced from Alhagi

(Penjerapan Para Nitro-fenol dengan Karbon Aktifan Dihasilkan daripada Alhagi)

Ghufran Muafaq Abd-Hadi & Sami D. Salman*

ABSTRACT

This manuscript has present an experimental study for Para Nitro-phenol (PNP) removal from aqueous solution using by physiochemical Alhagi activated carbon (AAC). AAC was characterized using SEM to investigate surface morphology and BET to estimate the specific surface area. The best surface area of AAC was found to be 641.6 m^2/gm which was obtained at 600ºC activation temperature and impregnation ratio of 1:1 of KOH. The investigated factors for PNP ions adsorption and their ranges such as initial concentration (10-50 mg/L), adsorption time (30-210 min), temperature (20-50ºC) and solution pH (4-10). Isotherm of adsorption and its kinetics were studied. The adsorption process was modeled statistically by an empirical model. The equilibrium data were fitted to the Langmuir and Freundlich isotherm models and the data found to be well represented by Langmuir isotherm. Pseudo- first order and pseudo- second order kinetic equations were utilized to study adsorption kinetics. It is found that the PNP adsorption on AAC fitted pseudo- second more adequately and the best removal efficiency was found to be 97.59%.

Keywords: Adsorption; activated carbon; alhagi; PNP; physiochemical activation

ABSTRAK

Kertas ini telah membentangkan satu kajian uji kaji untuk penyingkiran para Nitro-fenol (PNP) daripada larutan akueus menggunakan karbon aktifan fiziokimia Alhagi (AAC). AAC telah dicirikan dengan menggunakan SEM untuk mengkaji permukaan morfologi dan BET untuk menganggar bahagian permukaan tertentu. Kawasan permukaan terbaik AAC ialah 641.6 m^2/gm yang diperoleh pada suhu pengaktifan 600ºC dan nisbah impregnasi 1:1 KOH. Faktor yang dikaji bagi penjerapan ion PNP dan julatnya seperti kepekatan awal (10-50 mg/L), masa penjerapan (30-210 min), suhu (20-50ºC) dan larutan pH (4-10). Isoterma penjerapan dan kinetik telah dikaji. Proses penjerapan ini dimodelkan secara statistik oleh model empirik. Data keseimbangan disuaikan kepada model isoterma Langmuir dan Freundlich dan data ini didapati diwakili dengan baik oleh isoterma Langmuir. Persamaan kinetik tertib pertama pseudo dan tertib kedua pseudo telah digunakan untuk mengkaji penjerapan kinetik. Didapati bahawa penjerapan PNP pada AAC lebih sesuai untuk pseudo kedua dan kecekapan penyingkiran terbaik adalah pada 97.59%.

Kata kunci: Alhagi; karbon aktifan; penjerapan; PNP pengaktifan fiziokimia

Introduction

Due to the wide range and the exaggerated uses of organic solvents, oxidizing agents, phenols, heavy metals in industry, and there was accumulation in the environment, which led some ecosystems to deteriorate. When organic pollutants are discharged into ecosystem they cause the waters to be odorous with obnoxious taste (Md. Ahmaruzzaman 2008). Industrial wastewaters cannot be discharged without treatment, because they impose a crucial effect on humans and animals. Chemicals, plastics, dyes manufacturing industries and coal thermal processing release invariable concentrations of phenols and their derivatives into water bodies, many of these phenolic compounds are carcinogenic even at low concentrations (Abdelkreem 2013).

Phenols are one of the most lethal pollutants of surface and ground waters. Industrial effluents are the major source. Because almost all of phenols take a long time to degrade into harmless components (Muftah et al. 2010), therefore; reduction of phenols concentrations before discharging them into rivers had become a necessity, otherwise they could be harmful to the health and/or reduce drinking water quality (Mandal & Sudip Kumar 2019). *p*-Nitro phenol (PNP) is an important fine chemical intermediate, serving as a precursor of pharmaceuticals and pesticides (Tang et al. 2015, 2007). Diesel fuel and gasoline exhaust also contain PNP that enters water body through rainwater (Mishra et al. 2019). PNP has been selected as one of the persistent, bio-accumulative and toxic (PBT) chemicals by the US Environmental Protection Agency (Gowthami & Sharpudin 2016). According to the US Environmental Protection Agency (USEPA), Phenols have been registered as priority pollutants with a permissible limit of 0.1 mg/L in wastewater (Muftah et al. 2010). The drinking water guideline value recommended by World Health Organization (WHO) and Iraqi standard regulation is 0.01 and 0.015 mg/L. As a result of toxicity of this element and its compounds, removal has become an important priority.

Several techniques were developed to reduce PNP levels from water including coagulation (Iwagaki et al. 2019; Lee 2019), membrane filtration (Bódalo et al. 2009; Zagklis et al. 2015), chemical precipitation (Naghmeh Sadat & Sabbaghi 2017; Sridhar et al. 2018), reverse osmosis (Al-Obaidi et al. 2018; Mujtaba 2017), chemical oxidation (Liu et al. 2019; Zambrano & Min 2019), ion-exchange (Javier et al. 2017; Víctor-Ortega et al. 2016) and immobilization (Bing et al. 2019; Li et al. 2019). But these methods are generally require high cost and produce more lethal products (Kulkarni et al. 2013). Many researchers have used different methods adsorption phenolic compounds on activated carbon as effective adsorbents for the removal of phenolic compounds from; industrial wastewater due to its high removal efficiency and highly adsorption capacity (Ayranci 2005; Brasquet & Le Cloirec 1999; Chern & Chien 2002; Daifullah & Girgis 1998; Daoud et al. 2019; Nouri 2004; Wolborska 1989). The high capacity of activated carbon products for adsorption is associated to the characteristics carbon structure and their porous shape that offers high surface area.

The significant cost of the commercial activated carbon that used for pollutants adsorption has promoted the researchers to fond low-cost activated carbon for pollutants adsorption from the wastewater at low operating cost as compared with that commercially used. Thus, agricultural source, such as date-pit and olive mill waste were used foe phenol removal from aqueous solutions (Abdelkreem 2013; Muftah et al. 2010). The main objective of this research is to explore new natural plant source namely Alhaji as a low-cost material to produce activated carbon due to their carbonaceous contents and its abundance to remove phenol. From aquake solution.

Materials and Methods

adsorbate

Technical grade 4-Nitrophenol powder ($O_2NC_6H_4OH$) of 99.6% purity provided by Sigma Aldrich, Germany was used to prepare stock solution. All solutions were prepared using distilled water. A stock of 1000 mg/L was prepared by adding (1) gm of PNP to a liter of DW, dilution law was used to prepare the required concentrations. 0.1 M HNO_3 and 0.1 M NaOH were used to adjust the pH. All chemicals and gases used in this research are illustrated in Table 1.

preparation and characterization of activated carbon

Alhagi was collected from University of Baghdad, Baghdad, Iraq. The preparation method of Alhagi activated carbon is concise in Figure 1. The conditions that were used in Alhagi charring were obtained from Moreno-piraján (Moreno-piraján et al. 2010). The surface area was analyzed using Brunaure-Emmett-Teller (BET: HORIBA, SA-900 series, USA) through nitrogen adsorption isotherm at 77 K. In order to determine the shape of CBAC surface, the samples were scanned using Scanning Electron Microscope (TESCAN, Vega III, Czech Republic).

Design of Experiments

Experimental design usually used to efficiently map the set of experiments was conducted to understand the effect of the factors and/or model the relationship between response and factors with a minimum of experiments (Massart & Vandeginste 1991). A fractional factorial design was chosen as a method to optimize the production of AAC, while Taguchi design was utilized in the adsorption optimization and modeling of due to its efficiency compared to other methods and its robustness. STATISTICA 10 (StatSoft, Inc. USA) was used to design the set of experiments. Table 2 shows the fractional factorial design for 2 factors with mixed levels for AAC preparation and Table 3 shows the L16 orthogonal Taguchi array (4 factors, 4 levels) for PNP adsorption process.

Batch Equilibrium Studies

Bach mode adsorption experiments were conducted by adding specific amount of adsorbent to a 100 mL PNP solution contained in a 125 mL capped plastic containers. The containers were placed in an isothermal shaker (JSSI-300CL, JSR, Korea) at an agitation speed of 180 rpm. The remaining concentration of PAP in each sample after adsorption at different times was determined by UV- Visible absorption spectroscopy (Shimadzu AA1600, Japan). All samples were filtered from the adsorbent with Whatman filter paper to make it carbon free. The PNP concentration adsorbed on AAC was predicted according to:

$$q_e = \frac{(C_o - C_e)V}{W} \quad (1)$$

where q_e is the adsorption capacity at equilibrium (mg/g); C_o and C_e are the concentrations at initial and equilibrium conditions (mg/L) for PNP solution, respectively; V is the volume (L); and W is the weight (g) of AAC.

Adsorption Process Modeling

After adsorption batch experiments were run, the equilibrium concentrations (C_e) were used to form a mathematical model that represent the adsorption process. This model relates C_e as a response with the investigated factors which are: initial concentration, contact time, temperature and solution pH. STATISTICA 10 (StatSoft, Inc. USA) was utilized to form the model by nonlinear estimation method. This model was used to generate the equilibrium concentration at various conditions; these results were used in adsorption isotherm fitting, kinetics study and adsorption thermodynamics.

TABLE 1. Chemicals and gases

Name	Formula	Assay (%)	Source or company	Usage
Nitrogen	N_2	99.9	Local	Inert gas to prevent raw material combustion
Potassium Hydroxide pellet	KOH	85	Himedia, India	Chemical activating agent
Carbon dioxide	CO_2	99.9	Local	Physical activating agent
Hydrochloric acid	HCl	2N	England	Washing and Neutralizing of AC
4-Nitrophenol	$O_2NC_6H_4OH$	99,6	Sigma-Aldrich	PNP source
Nitric acid	HNO_3	70	J. T.Baker, Holland	Solution pH adjustment
Sodium hydroxide	NaOH	99.5	DIDACTIC, Spain	Solution pH adjustNumber

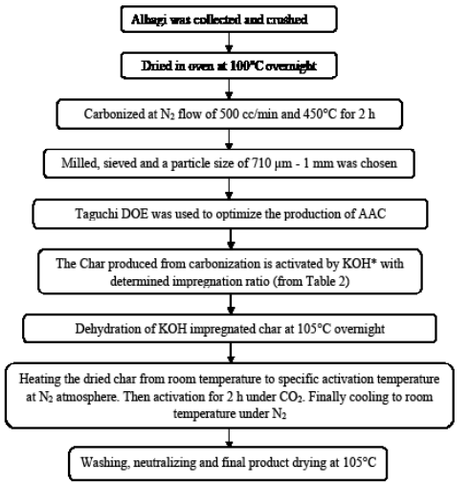

FIGURE 1. Schematic diagram for the AAC preparation steps

TABLE 2. Fractional factorial. Design of AAC optimization

Number	IR	Activation temperature (°C)
1	1:1	500
2	1:1	550
3	1:1	600
4	1:1	650
5	1:2	500
6	1:2	550
7	1:2	600
8	1:2	650
9	1:3	500
10	1:1	550
11	1:3	600
12	1:3	650

Adsorption Isotherm

Two isotherm models (Langmuir and Freundlich) were used to fit the equilibrium data. The linear form of the Langmuir (1916) model is:

$$\frac{1}{q_e} = \frac{1}{q_m} + \frac{1}{(K_a q_m)} \frac{1}{C_e} \quad (2)$$

where C_e (mg/L) is the concentration of PNP at equilibrium; q_e (mg/g) the equilibrium adsorption capacity; q_m the adsorption capacity for a complete monolayer (mg/g); K_a (L/mg) is the constant of adsorption equilibrium. The linear form of Freundlich (1925) isotherm is:

$$\ln q_e = \ln K_F + \left(\frac{1}{n}\right) \ln C_e \quad (3)$$

where K_F (mg/g) and n are the Freundlich constants.

KINETIC STUDIES

The adsorption rate constants were predicted from the pseudo-first-order and pseudo-second-order equations. For the pseudo-first-order, the Lagergren (Ho 2016) expression was used:

$$\log(q_e - q_t) = \log q_e - \frac{k_1 t}{2.303} \quad (4)$$

where q_e and q_t (mg/g) are the adsorption capacities at equilibrium and at time t (min), respectively, and k_1 (1/min) is the adsorption constant. The linear form of the pseudo-second-order (Boehm 1994) reaction can be given by:

$$\frac{t}{q_t} = \frac{1}{k_2 q_e^2} + \frac{1}{q_e} t \quad (5)$$

where the adsorption capacity of equilibrium (q_e) and the constant of second order k_2 (g/mg h) can be determined experimentally from the intercept and slope of t/qt versus t plot.

Results and Discussion

AAC PRODUCTION AND OPTIMIZATION

The complete design array for the surface area and yield as responses of AAC preparation with two factors, temperature of activation and impregnation ratio (IR) (char: KOH wt: wt) from the experiments that were conducted are shown in Table 4.

It is found that in AAC preparation the SSA decreases as IR rises, the SSA decreased, this was probably due to excessive potassium hydroxide molecules decomposing

TABLE 3. Taguchi DOE (L16 array) of PNP adsorption experiments

Number	Initial concentration (mg/L)	Contact time (min)	Temperature (°C)	Solution pH
1	10	30	20	4
2	10	90	30	6
3	10	150	40	8
4	10	210	50	10
5	20	30	30	8
6	20	90	20	10
7	20	150	50	4
8	20	210	40	6
9	30	30	40	10
10	30	90	50	8
11	30	159	20	6
12	30	210	30	4
13	50	30	50	6
14	50	90	40	4

into metal. As a result, metal deposition on the already developed pores might have occurred and led to reduction of the surface area (Azry et al. 2014). The relation between SSA, activation temperature and impregnation ratio as shown in Figure 2.

Regarding the activation temperatures, it is perceived that as temperature rises from 500C° to 600°C, the SSA increases with it. These results showed that as the activation temperature increases, the structure has a tendency to become micro-porous. That's due to that porosity is formed by KOH evaporation, therefore; as temperature increases, more KOH evaporates which leads to micro porosity enhancement (Chandra et al. 2007). On the other hand, SSA decreased at 650°C, this is probably because high activating temperatures caused pore explosion that led to lower values of specific surface area (Nayak et al. 2017).

In general, the AAC yield was found to be inversely proportional to both temperatures of activation and IR. As temperature elevate more volatile components will be released due to intensified dehydration and elimination reaction that increase C-KOH and C-CO2 reactions rates, which causes lower yield (Danish et al. 2014). As the IR value rises, KOH amount increases which leads to oxidation process promotion causing the carbon atoms gasification reaction to become more dominant, therefore; more weight of carbon would be lost (Sudaryanto et al. 2006). The relation between yield, activation temperature and impregnation ratio is shown in Figure 3.

SEM AND BET ANALYSIS

Figure 4 shows the SEM images of Alhagi (a) and AAC (b). It can be noticed that AAC surface has developed pores in

TABLE 4. Preparation of AAC experimental design array and the results for SSA and yield

Run	AAC preparation responses		AAC preparation variables	
	IR	Activation temperature (°C)	Specific surface area (m2/gm)	Yield (%)
1:1	1	85.63	301.59	500
1:1	2	73.47	534.20	550
1:1	3	70.93	641.60	600
1:1	4	61.50	461.30	650
1:2	5	80.46	277.41	500
1:2	6	67.49	409.10	550
1:2	7	65.19	522.17	600
1:2	8	55.62	382.46	650
1:3	9	70.59	160.67	500
1:3	10	60.62	291.35	550
1:3	11	58.95	410.52	600
1:3	12	50.47	349.45	650

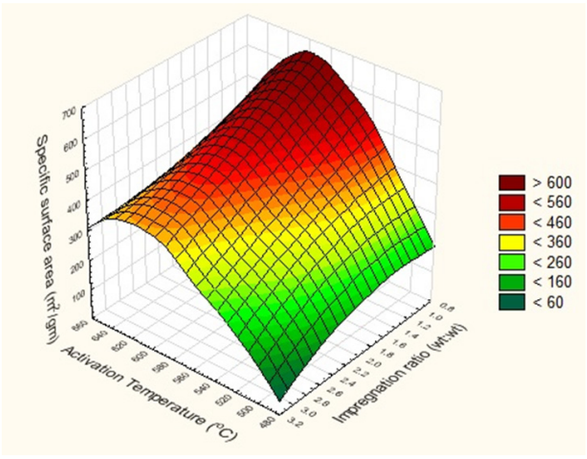

FIGURE 2. Effect of activation temperature and impregnation ratio on SSA

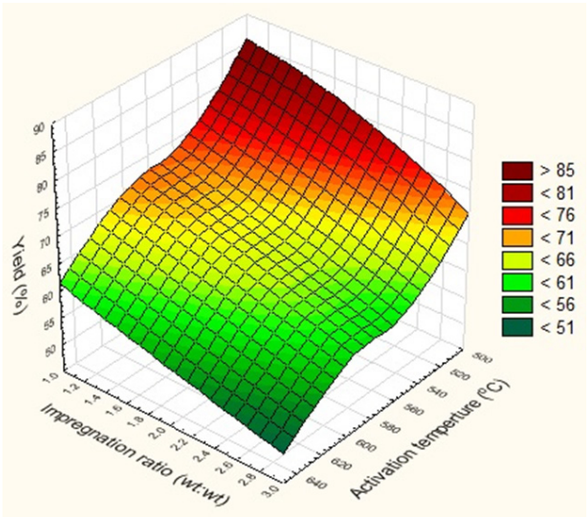

FIGURE 3. Effect of activation temperature and impregnation ratio on yield

TABLE 5. Batch adsorption experiments and their response

Initial concentration (mg/L)	Time (min)	Temperature (°C)	pH	Equilibrium concentration (mg/L)
10	30	20	4	5.979
10	90	30	6	2.689
10	150	40	8	3.170
10	210	50	10	1.296
20	30	30	8	4.329
20	90	20	10	2.028
20	150	50	4	4.137
20	210	40	6	5.177
30	30	40	10	0.788
30	90	50	8	3.565
30	150	20	6	7.810
30	210	30	4	6.693
50	30	50	6	14.939
50	90	40	4	18.956
50	150	30	10	6.114
50	210	20	8	6.387

which there is a good probability for PNP to be adsorbed. The BET surface area was 641.6 m^2/g. Pore diameter in average was 2.435 µm, indicating that it was in the macroporous region according to the International Union of Pure and Applied Chemistry (IUPAC). The pores are classified as micro pores (<2 nm diameter), mesoporous (2-50 nm diameter) and macro pores (>50 nm diameter) (Padmaja Sudhakar & Soni 2018). The AAC has high surface area which makes it more efficient for the removal of PNP. The high SSA of the AAC was a result of the used technique of activation. The activation process involved chemical and physical activating agents which are KOH and CO_2, respectively. However, the developed pores during carbonization enhanced the surface area by diffusing more CO_2 and KOH molecules inside the pores, therefore; the reaction between KOH-carbon and CO_2-carbon promoted leading to more pores in the activated carbon.

Experimental Design and Empirical Model

The following set of experiments that designed by Taguchi method and their results are shown in Table 5.

In order to obtain the empirical model for the adsorption process the results from Taguchi experimental design was used. Y is the response variable, the obtained model with its four factors and their interaction is represented by:

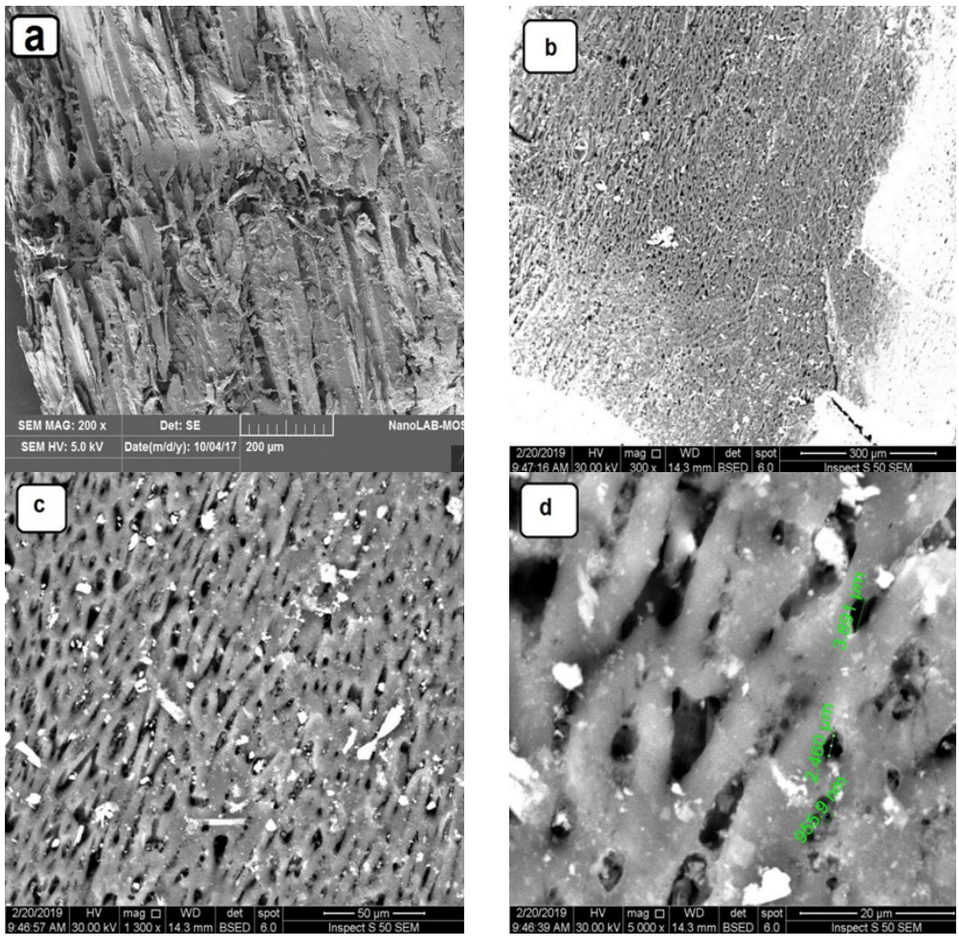

FIGURE 4. SEM images, a) precursor b-d) AAC at different magnifications

TABLE 6. Model coefficients, standard error and terms p- values

Linear coefficient and second- order interaction terms	Estimate	Standard error	p-value
b_1	0.49888	0.1880	0.0118
b_2	-0.05360	0.0350	0.0272
b_3	0.23712	0.1910	0.0342
b_4	0.19799	1.3500	0.0490
b_{12}	-0.00100	0.0007	0.0270
b_{13}	0.00214	0.0041	0.0650
b_{14}	-0.03607	0.0108	0.0792
b_{23}	0.00103	0.0009	0.0373
b_{24}	0.00882	0.0048	0.021
b_{34}	-0.00860	0.0121	0.0549
b_{11}	-0.00030	0.0029	0.0926
b_{22}	-0.00002	0.0001	0.0802
b_{33}	-0.00643	0.0024	0.0119
b_{44}	-0.10338	0.0994	0.0408

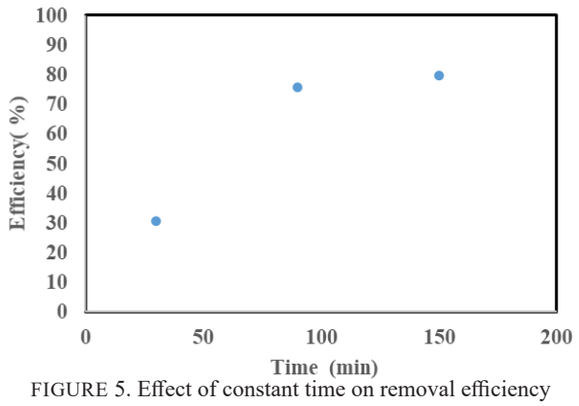

FIGURE 5. Effect of constant time on removal efficiency

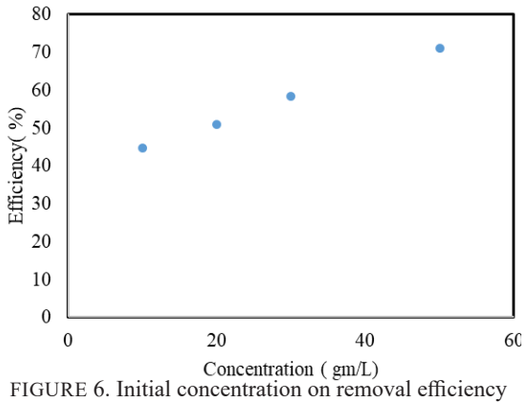

FIGURE 6. Initial concentration on removal efficiency

$$Y = b_o+b_1 X_1+b_2 X_2+b_3 X_3+b_4 X_4+b_{12} X_1 X_2 +b_{13} X_1 X_3+b_{14} X_1 X_4+b_{23} X_2 X_3+b_{24} X_2 X_4 +b_{34} X_3 X_4+b_{11} X^2_1+b_{22} X^2_2+b_{33} X^2_3+b_{44} X^2_4 \quad (6)$$

where b_0, b_1, b_2, b_3 and b_4 are the linear coefficients, b_{12}, b_{13}, b_{14}, b_{23}, b_{24} and b_{34} are the second-order interaction terms, b_{11}, b_{22}, b_{33} and b_{44} are the quadratic terms of each factor. X_1, X_2, X_3 and X_4 are the coded terms of initial chromium concentration, time, temperature and pH, respectively.

The estimated values of the model coefficient, standard error of each model term and its p value are shown in Table 6.

As can be seen from Table 6, b_{13}, b_{14}, b_{34}, b_{11}, and b_{22} have insignificant effect on model accuracy due to their p values which are larger than 0.05.

Effects of Factors

a- effect of contact time and PNP initial concentration

The influence of adsorption time on PNP ions adsorbed by AC was investigated as shown in Figure 5. It is observed that the PNP ions removal efficiency by AC increased with the initial PNP ion concentration. The adsorption was fast at the initial stage because of the high driving force which induced the PNP ions to transfer rapidly from the bulk solution to the surface of AC (Abdelkreem 2013). As time passed, more active sited were occupied, which means less free active sites on the surface. Alongside with the declined driving force that made the adsorption to take more time to reach equilibrium, because PNP ions slowly diffused to the intra-particle pores of the adsorbent (Xue et al. 2013). Thus, the adsorption rate was decreased.

It is also clear from Figure 6 that removal efficiency improved as the initial concentration of PNP. Because of the increasing driving force of the concentration gradient (Xue et al. 2013).

b- effect of pH and temperature

The solution initial pH is the most significant factor to investigate the adsorption characteristic of an adsorbent because it affects not only surface charge of the adsorbent, but also the ionization degree and adsorbate speciation (Ahmaruzzaman & Sharma 2005). The effect of initial solution pH on PNP ion removal by AAC is presented in Figure 7. As it can be observed from Figure 7 that the efficiency increases as pH value increases in the range of 2-8, on the other hand removal efficiency declines as pH value reach to 10. This result can be clarified by the functional group types that existed on the adsorbent surface beside the phenol speciation due to pH change. As initial pH value is within the acidic region, more positive functional groups are exposed, these positive functional groups will attract more phenol ions, that will lead to higher removal efficiency (Muataz Ali 2014), but when pH value increase above 8 negative functional groups are the dominant groups, this may be led to a creation of repulsive forces between the phenol ions and the adsorbent surface (Ahmaruzzaman & Sharma 2005). Moreover, phenolic compounds tend to form negatively charged ionized salts that precipitate in alkali pH range (Yang et al. 2015). The removal efficiency for PNP, which is a weak acid (pKa = 7.13), peaked at pH = 8 and the adsorbed PNP was lesser at pH = 10 due to the repulsive forces that dominate at higher pH (Moreno-castilla 2004).

Adsorption process is an exothermic process, due to the fact that adsorption causes the residual forces on the surface of the adsorbent to decrease, which leads to lower surface energy. The difference in surface energy is released as heat (Ruthven & Wiley 1985). The dissipation (despite its small amount) through cooling would enhance the adsorption efficiency Figure 8 illustrates the inversely proportional relation between temperature and efficiency of adsorption. As it can be seen from Figure 8 that PNP adsorption on AC is exothermic process.

Adsorption Isotherm Studies

The correlation between bulk solution concentration of sorbate and the amount of adsorbed PNP on AAC unit at equilibrium conditions is described functionally by the isotherms of adsorption. To understand the behavior of PNP ions in the solution - AAC interphase, the adsorption isotherm was studied. Usually adsorption isotherm analysis is conducted to find the fitter model to be used in equipment

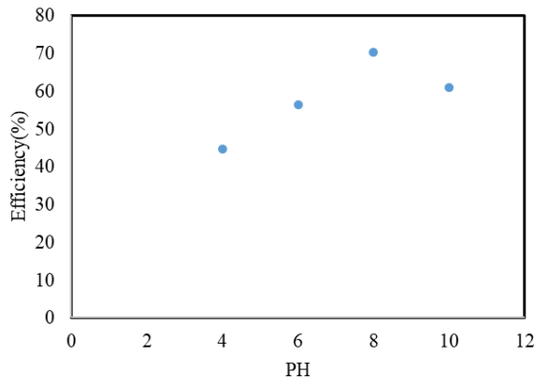

FIGURE 7. The effect of initial PH on adsorption efficiency

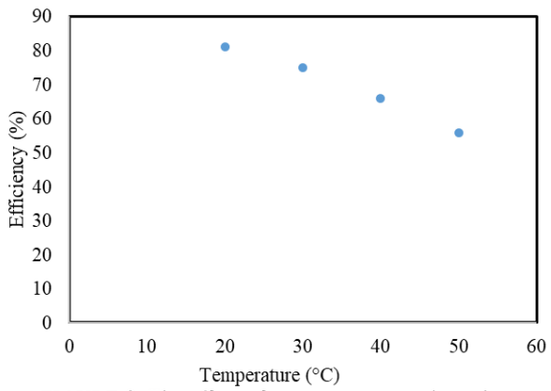

FIGURE 8. The effect of temperature on adsorption efficiency

TABLE 7. Values of Freundlich and Langmuir constants for PNP adsorption on AAC

	Langmuir			Freundlich		
Temperature (C°)	KL (L/mg)	qm (mg/g)	R^2	KF (mg/g)	n	R^2
20	0.171	27.45	0.9691	1.442	1.262	0.907
30	0.081	24.12	0.9714	3.172	1.463	0.960
40	0.037	23.35	0.9811	0.409	0.831	0.908
50	0.021	21.09	0.9572	0.173	0.787	0.922

TABLE 8. Comparison of the pseudo-first and pseudo-second order rate constants, and calculated and experimental qe values PNP adsorption on AAC for various initial concentrations

Initial concentration (mg/L)		Pseudo-first order			Pseudo-second order		
	qe,exp (mg/g)	K_1 (1/min)	qe,cal (mg/g)	R_2	K_2 (g/mg min)	qe,cal (mg/g)	R_2
10	3.935	0.011	2.758	0.974	0.0316	3.411	0.991
20	7.3403	0.0062	4.626	0.938	0.0137	7.189	0.998
30	10.368	0.0052	6.299	0.933	0.0146	9.820	0.991
40	13.385	0.0045	7.965	0.931	0.0158	15.456	0.999
50	17.254	0.0045	9.281	0.897	0.0265	18.903	0.999

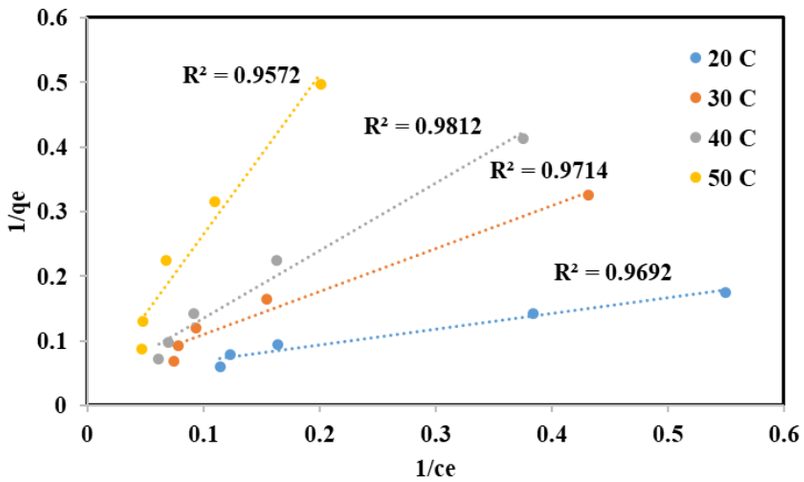

FIGURE 9. Adsorption data fitted into Langmuir isotherm at temperature range of (20-50°C)

design purposes. Table 7 summarizes the capacities of adsorption for a monolayer coverage as implied by Langmuir model with the two isotherms constants and their correlation coefficients at 20, 30, 40 and 50ºC. As it can be observed that Langmuir model fitted adsorption data of PNP more adequately due to higher R^2 values at all the mentioned temperature range, where R^2 was more than 0.97. Fitting Langmuir isotherm refers to the homogeneous surface energies and refers to the formation of a monolayer of PNP on the surface of the produced activated carbon (Karunarathne & Amarasinghe 2013; Mishra et al. 2019). Figure 9 shows the plot of $1\backslash C_e$ versus $1\backslash q_e$ with temperature range of 20-50ºC. Other studies had also confirmed the same results (Álvarez et al. 2005; Padmaja Sudhakar & Soni 2018).

Kinetics Studies

To figure out the mechanism that controls the adsorption of PNP on AAC, such as physical interactions and chemical reaction, pseudo-first-order and pseudo-second-order equations were utilized to model the kinetics of adsorption. The comparison between experimental and calculated concentration of equilibrium and correlation coefficients were used to evaluate kinetics equations fitting. As the difference between experimental equilibrium concentration (qe,exp) and calculated equilibrium concentration (qe,cal) get smaller and R2 goes to unity, the kinetic equation represents the adsorption more accurately. The kinetics was studied at different initial concentration of chromium. PNP adsorption obeyed pseudo-second order more clearly compared to pseudo-first order. Pseudo-first order and pseudo-second order adsorption rate constants, calculated and experimental qe values for different initial concentration of PNP are summarized in Table 8. Other researches had confirmed the same results (Larous & Meniai 2012; Thue et al. 2016).

Conclusion

In this study, Alhagi active carbon showed an encouraging prospect in PNP adsorption from aqueous solution over a wide range of conditions, the optimum removal efficiency was 97.59%. Highest SSA of AAC was 641.6 m^2/g at activation temperature of 600ºC and IR of 1:1. Langmuir and Freundlich isotherm models were utilized to fit the data of equilibrium and the equilibrium data for AAC were best represented by the Langmuir isotherm at different temperatures with R^2 values more than 0.9572. The kinetics of adsorption followed the pseudo second- order kinetic model at various initial PNP concentration, pseudo-second order kinetic model produced highest R^2 values (larger than 0.99). Due to the high range of removal efficiency, AAC can be used as a cost effective, inexpensive substitute to the commercial activated carbons.

Acknowledgements

The author gratefully acknowledges the technical support from the University of Baghdad, Al-Khwarizmi College of Engineering, and Department of Biochemical Engineering.

References

Abdelkreem, M. 2013. Adsorption of phenol from industrial wastewater using olive mill waste. *APCBEE Procedia* 5: 349-357. https://doi.org/10.1016/j.apcbee.2013.05.060.

Ahmaruzzaman, M. & Sharma, D.K. 2005. Adsorption of phenols from wastewater. *Journal of Colloid and Interface Science* 287: 14-24. https://doi.org/10.1016/j.jcis.2005.01.075.

Al-Obaidi, M. A., Jarullah, A. T., Kara-Zaïtri, C. & Mujtaba, I. M. 2018. Simulation of hybrid trickle bed reactor-reverse osmosis process for the removal of phenol from wastewater. *Computers and Chemical Engineering Received* 113: 264-273.

Álvarez, P. M., García-araya, J. F., Beltrán, F. J., Masa, F.J. & Medina, F. 2005. Ozonation of activated carbons: Effect on the adsorption of selected phenolic compounds from aqueous solutions. *Journal of Colloid and Interface Science* 283: 503-512. https://doi.org/10.1016/j.jcis.2004.09.014.

Arunima Nayak, Brij Bhushan, Vartika Gupta. & P. Sharma. 2017. Chemically activated carbon from lignocellulosic wastes for heavy metal waste-water remediation: Effect of activation conditions. *Journal of Colloid and Interface Science* 493: 228-240. https://doi.org/10.1016/j.jcis.2017.01.031.

Ayranci, E. O. D. 2005. Sorption behaviors of some phenolic compounds onto high specific area activated carbon cloth. *J. Hazard. Mater.* B124: 125-132.

Azry Borhan, Mohd Faisal Taha & Athirah Amer Hamzah 2014. Characterization of activated carbon from wood sawdust prepared *via* chemical activation using potassium hydroxide. *Advanced Materials Research* 832: 132-137. https://doi.org/10.4028/www.scientific.net/AMR.832.132.

Bing, H., Sharadwata, P. & Danquah, M. K. 2019. An overview of immobilized enzyme technologies for dye, phaenolic removal from wastewater. *Biochemical Pharmacology* 7(2): 102961. https://doi.org/10.1016/j.jece.2019.102961.

Bódalo, A., Gómez, E., Hidalgo, A.M., Gómez, M., Murcia, M. D. & López, I. 2009. Nanofiltration membranes to reduce phenol concentration in wastewater. *DES* 245(1-3): 680-686. https://doi.org/10.1016/j.desal.2009.02.037.

Boehm, H. P. 1994. Some aspects of the surface chemistry of carbon blacks and other carbons. *Carbon* 32(5): 759-769. https://doi.org/10.1016/0008-6223(94)90031-0.

Brasquet, C. E. S. & Le Cloirec, P. 1999. Removal of phenolic compounds from aqueous solution by activated carbon cloths. *Water Science Technology* 39: 201-205.

Chandra, T. C., Mirna, M. M., Sudaryanto, Y. & Ismadji, S. 2007. Adsorption of basic dye onto activated carbon prepared from durian shell: Studies of adsorption equilibrium and kinetics. *Chemical Engineering Journal* 127(1-3): 121-129. https://doi.org/10.1016/j.cej.2006.09.011.

Chern, J. M. & Chien, Y. W. 2002. Adsorption of nitrophenol onto activated carbon: Isotherms and breakthrough curves. *Water Research* 36: 647-655.

Daifullah, A. A. M. & Girgis, B. S. 1998. Removal of some substituted phenols by activated carbon obtained from agriculture waste. *Water Research* 32: 1169-1177.

Danish Mohammed, Rokiah Hashim, M. N. Mohamad Ibrahim. & Othman Sulaiman. 2014. Optimized preparation for large surface area activated carbon from date (*Phoenix dactylifera* L.) stone biomass. *Biomass and Bioenergy* 61(320): 167-178. https://doi.org/10.1016/j.biombioe.2013.12.008.

Freundlich, H. 1925. Capillary and colloid chemistry. Translated by Hatfield, H. S. *J. Phys. Chem.* 57: 385-470.

Gowthami, R. & Sharpudin, J. 2016. Removal of phenol from textile wastewater using natural adsorbent. *International Journal of Science, Engineering and Technology Research* 5(4): 1157-1161.

Ho, Y-S. 2016. Comments on using of "pseudo-first-order model". *Journal of Taiwan Institute of Chemical Engineers* http://dx.doi.org/10.1016/j.jtice.2016.06.032

Iwagaki, F., Ogando, B., De Aguiar, C. L., Napolitano Viotto, V., José Heredia, F. & Hernanz, D. 2019. Removal of phenolic, turbidity and color in sugarcane juice by electrocoagulation as a sulfur-free process. *Food Research International* 122: 643-652.

Javier M. Ochando-pulido, Ruben González-Hernández & Antonio Martinez-Ferez. 2017. On the effect of the operating parameters for two-phase olive-oil washing wastewater combined phenolic compounds recovery and reclamation by novel ion exchange resins. *Separation and Purification Technology* 195: 50-59.

Karunarathne, H. D. S. S. & Amarasinghe, B. M. W. P. K. 2013. Fixed bed adsorption column studies for the removal of aqueous phenol from activated carbon prepared from sugarcane bagasse. *Energy Procedia* 34: 83-90. https://doi.org/10.1016/j.egypro.2013.06.736.

Kulkarni, S. J., Tapre, R. W., Patil, S. V. & Sawarkar, M. B. 2013. Adsorption of phenol from wastewater in fluidized bed using coconut shell activated carbon. *Procedia Engineering* 51(2012): 300-307. https://doi.org/10.1016/j.proeng.2013.01.040.

Langmuir, I. 1916. The constitution and fundamental properties of solids and liquids. *Journal of the Franklin Institute* 183(1): 102-105.

Larous, S. & Meniai, A. H. 2012. The use of sawdust as by product adsorbent of organic pollutant from wastewater: Adsorption of phenol. *Energy Procedia* 18: 905-914. https://doi.org/10.1016/j.egypro.2012.05.105.

Lee Soo Min, Jeong Hanseob, Lee Jaejung. & Young Min Ju. 2019. Using electro-coagulation treatment to remove phenolic compounds and furan derivatives in hydrolysates resulting from pilot-scale supercritical water hydrolysis of Mongolian oak. *Renewable Energy* 138: 971-979.

Li Jinlong, Chen Xiangyang, Xu Dongfeng. & Pan Kai. 2019. Ecotoxicology and environmental safety immobilization of horseradish peroxidase on electrospun magnetic nano fibers for phenol removal. *Ecotoxicology and Environmental Safety* 170: 716-721. https://doi.org/10.1016/j.ecoenv.2018.12.043.

Liu Yi-Hung, Huang Wei-Jin. & Wang Chih-Ta. 2019. Photoelectrocatalytic oxidation of phenol by UV-assisted electrogenerated Ce (IV) in aqueous solution. *Journal of the Taiwan Institute of Chemical Engineers* 102: 218-224.

Mandal Ashanendu. & Sudip Kumar Das. 2019. Phenol adsorption from wastewater using clarified sludge from basic oxygen furnace. *Journal of Environmental Chemical Engineering* 7(4): 103259.

Md. Ahmaruzzaman. 2008. Adsorption of phenolic compounds on low-cost adsorbents: A review. *Advances in Colloid and Interface Science* 143: 48-67. https://doi.org/10.1016/j.cis.2008.07.002.

Massart, L. & Vandeginste, B. 1991. *Chemometrics and Qualimetrics in Chemical Engineering.* New Jersey: Princeton Press.

Mishra Shubham, Swati Singh, Shalu Rawat. & Jiwan Singh. 2019. Corn husk derived magnetized activated carbon for the removal of phenol and para-nitrophenol from aqueous solution: Interaction mechanism, insights on adsorbent characteristics, and isothermal, kinetic and thermodynamic properties. *Journal of Environmental Management* 246: 362-373.

Moreno-Castilla, C. 2004. Adsorption of organic molecules from aqueous solutions on carbon materials Q. *Carbon* 42: 83-94. https://doi.org/10.1016/j.carbon.2003.09.022.

Moreno-piraján, J. C., Gómez-Cruz, R., García-Cuello, V. S. & Giraldo, L. 2010. Binary system Cu(II)/Pb(II) adsorption on activated carbon obtained by pyrolysis of cow bone study. *Journal of Analytical and Applied Pyrolysis* 89: 122-128. https://doi.org/10.1016/j.jaap.2010.06.007.

Mounir Daoud, Oumessaâd Benturki, Girods, P., Donnot, A. & Fontana, S. 2019. Adsorption ability of activated carbons from *Phoenix dactylifera* rachis and *Ziziphus jujube* stones for the removal of commercial dye and the treatment of dyestuff wastewater mounir. *Microchemical Journal* 148: 493-502.

Muataz Ali Atieh. 2014. Removal of phenol from water different types of carbon - A comparative analysis. *Procedia-Social and Behavioral Sciences* 10: 136-141. https://doi.org/10.1016/j.apcbee.2014.10.031.

Muftah H. El-Naas, Sulaiman Al-Zuhair. & Manal Abu Alhaija. 2010. Removal of phenol from petroleum refinery wastewater through adsorption on date-pit activated carbon. *Chemical Engineering Journal* 162(3): 997-1005. https://doi.org/10.1016/j.cej.2010.07.007.

Mujtaba, I. M. 2017. Process: Model development based on experiment and simulation. *Journal of Water Process Engineering* 18(February): 20-28.

Naghmeh Sadat Mirbagheri & Samad Sabbaghi. 2017. A natural kaolin/γ-Fe2O3 composite as an efficient nano-adsorbent for removal of phenol from aqueous solutions. *Microporous and Mesoporous Materials* 259: 134-141.

Nouri, S. F. H. 2004. Adsorption of p-nitrophenol in untreated and treated activated carbon: *Adsorption* 10: 79-86.

Padmaja Sudhakar Pamidimukkala & Harnish Soni. 2018. Efficient removal of organic pollutants with activated carbon derived from palm shell: Spectroscopic characterisation and experimental optimisation *Journal of Environmental Chemical Engineering* 6(2): 3135-3149.

Ruthven, D. M. & Wiley, J. 1985. Principles of adsorption and adsorption inorganic ion exchange materials. *AiChE Journal* 31(3): 523-524.

Sridhar, R., Uma Ramanane, U. & Rajasimman, M. 2018. ZnO nanoparticles-synthesis, characterization and its application for phenol removal from synthetic and pharmaceutical industry wastewater. *Environmental Nanotechnology, Monitoring & Management* 10: 388-393.

Sudaryanto, Y., Hartono, S. B., Irawaty, W., Hindarso, H. & Ismadji, S. 2006. High surface area activated carbon prepared from cassava peel by chemical activation. *Bioresource Technology* 97: 734-739. https://doi.

org/10.1016/j.biortech.2005.04.029.

Tang Dengyong, Zheng Zheng, Lin Kui, Luan Jingfei. & Zhang Jibiao. 2007. Adsorption of p-nitrophenol from aqueous solutions onto activated carbon fiber. *Hazardous Materials* 143: 49-56. https://doi.org/10.1016/j.jhazmat.2006.08.066.

Tang Wenjing, Huang Huijuan, Gao Yajun, Liu Xiaoyao, Yang Xinyu, Ni Huijun. & Zhang Jianbin. 2015. Preparation of a novel porous adsorption material from coal slag and its adsorption properties of phenol from aqueous solution. *JMADE* 88: 1191-1200. https://doi.org/10.1016/j.matdes.2015.09.079.

Thue, P. S., Adebayo, M. A., Lima, E. C., Sieliechi, J. M., Machado, F. M., Dotto, G. L., Vaghetti, J. C. P. & Dias, S. L. P. 2016. Preparation, characterization and application of microwave-assisted activated carbons from wood chips for removal of phenol from aqueous solution. *Journal of Molecular Liquids* 223: 1067-1080. https://doi.org/10.1016/j.molliq.2016.09.032.

Víctor-Ortega, M. D., Ochando-Pulido, J. M. & Martínez-Ferez, A. 2016. Performance and modeling of continuous ion exchange processes for phenols recovery from olive mill wastewater. *Process Safety and Environmental Protection* 100: 242-251. https://doi.org/10.1016/j.psep.2016.01.017.

Wolborska, A. 1989. Adsorption on activated carbon of p-nitrophenol from aqueous solution. *Water Research* 23: 85-91.

Xue Guanghai, Gao Manglai, Gu Zheng, Luo Zhongxin. & Hu Zhaochao. 2013. The removal of p-Nitrophenol from aqueous solutions by adsorption using gemini surfactants modified montmorillonites. *Chemical Engineering Journal* 218: 223-231.

Yang Wenlan, Yu Zhou, Pan Bingcai, Lu, Lv. & Zhang Weiming. 2015. Simultaneous organic/inorganic removal from water using a new nanocomposite adsorbent: A case study of p-Nitrophenol and phosphate. *Chemical Engineering Journal* 268: 399-407. https://doi.org/10.1016/j.cej.2015.01.051.

Zagklis, D. P., Vavouraki, A. I., Kornaros, M. E. & Paraskeva, C.A. 2015. Purification of olive mill wastewater phenols through membrane filtration and resin adsorption/desorption. *Journal of Hazardous Materials* 285: 69-76. https://doi.org/10.1016/j.jhazmat.2014.11.038.

Zambrano, J. & Min, B. 2019. Comparison on efficiency of electrochemical phenol oxidation in two different supporting electrolytes (NaCl and Na2SO4) Using Pt/Ti Electrode. *Environmental Technology & Innovation* 15: 100382.

Biochemical Engineering Department
Al-khwarizmi College of Engineering
University of Baghdad
Baghdad 47024
Iraq

*Corresponding author; email: sami@kecbu.uobaghdad.edu.iq

Received: 19 August 2019
Accepted: 10 October 2019